



# **Regression Language Models for Code**

Yash Akhauri $^{*1,2}$ , Xingyou Song $^{*2}$ , Arissa Wongpanich $^2$ , Bryan Lewandowski $^2$  and Mohamed S. Abdelfattah $^1$ 

<sup>1</sup>Cornell University, <sup>2</sup>Google

\*Equal Contribution.

Code: https://github.com/google-deepmind/regress-lm

Dataset: https://huggingface.co/datasets/akhauriyash/Code-Regression

We study code-to-metric regression: predicting numeric outcomes of code executions, a challenging task due to the open-ended nature of programming languages. While prior methods have resorted to heavy and domain-specific feature engineering, we show that a single unified Regression Language Model (RLM) can simultaneously predict directly from text, (i) the memory footprint of code across multiple high-level languages such as Python and C++, (ii) the latency of Triton GPU kernels, and (iii) the accuracy and speed of trained neural networks represented in ONNX. In particular, a relatively small 300M parameter RLM initialized from T5Gemma, obtains >0.9 Spearman-rank on competitive programming submissions from APPS, and a single unified model achieves >0.5 average Spearman-rank across 17 separate languages from CodeNet. Furthermore, the RLM can obtain the highest average Kendall-Tau of 0.46 on five classic NAS design spaces previously dominated by graph neural networks, and simultaneously predict architecture latencies on numerous hardware platforms.

# 1. Introduction

Predicting metric outcomes from programs and source code is a valuable capability that has been intensely studied over the past few years, with varying names such as *performance prediction* and *static analysis*.

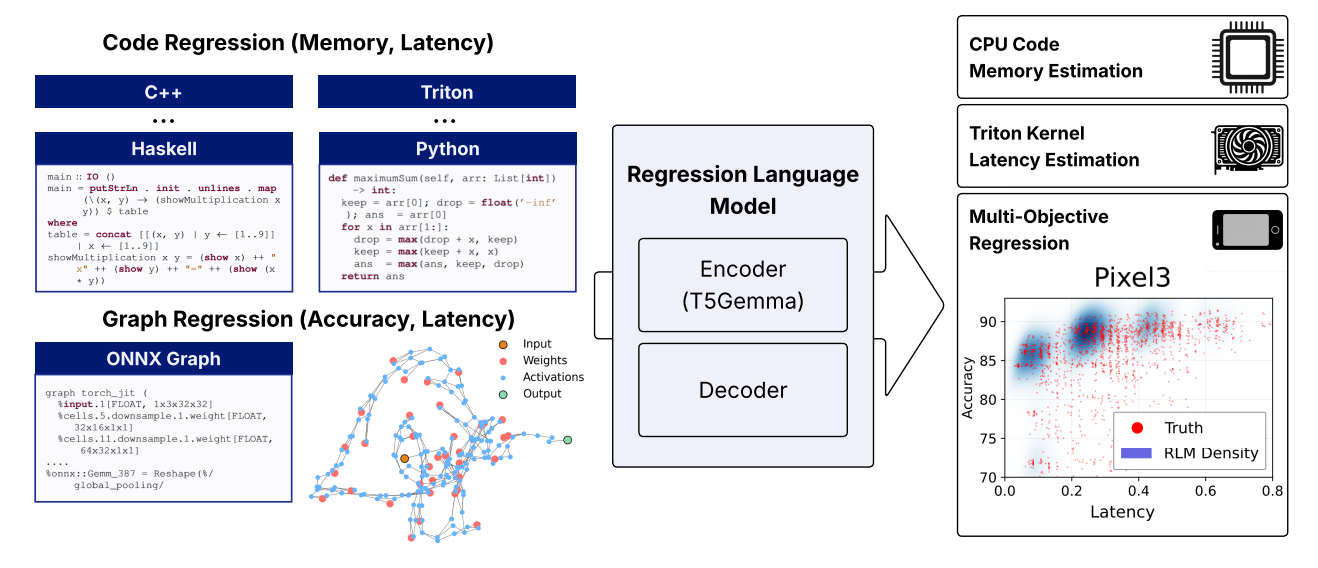


Figure 1 | A Regression Language Model (RLM) is able to simultaneously read code from many different languages and compilation levels, and predict metrics such as accuracy, memory, and latency.

The goal is to predict a useful metric, such as performance or efficiency, produced by executing a computation graph represented as either a high-level language such as Python, or low-level program

such as XLA. Achieving high precision predictions would naturally lead to more informed decision-making and better optimizations of all aspects in computing, including systems design, hardware manufacturing, and scientific discovery. However, one of the fundamental challenges in this domain is feature engineering, that is, learning highly accurate regression models over data from highly non-tabular, graph-based representations, which ideally should also be transferrable and reusable for new tasks.

Recent work (Song et al., 2024) have proposed a promising yet simple regression method, "text-to-text regression", based on small customized language models which can be trained over large amounts of (x, y) regression data represented as text. These *Regression Language Models* (RLMs) have shown promise over a variety of domains such as hyperparameter optimization (Song et al., 2024) and industrial systems (Akhauri et al., 2025), but up until now, it has been unknown whether such techniques can also be used for predictions over programs common to compilers and machine learning architectures. Below, we list our findings:

- A single, unified RLM initialized with a pretrained T5Gemma-S encoder can act as a general purpose code-to-metric regression model, by trainining over a large and diverse combination of regression data from GPU kernel programs, neural network architectures, and numerous different programming languages, as shown in Figure 1.
- Despite reading dense, complex ONNX representations for neural network graphs, RLMs are still able to remain competitive and even outperform state-of-the-art graph neural network (GNN)-based regression methods on standard neural architecture search (NAS) benchmarks. RLMs also naturally allow predicting multiple objectives such as latencies on different hardware.
- Comprehensive ablations demonstrate: (1) faster convergence curves when using model weights pretrained over standard language data and synthetic regression metrics, (2) decoder-based numeric outputs outperforming MSE-based regression heads, (3) improved regression with larger pretrained encoder sizes, and (4) important encoder settings such as tokenization and sequence length control.

Ultimately we hope this work paves the way for massively simplifying computational graph regression into a generic next-token prediction problem, aligning better with the modern large language model (LLM) paradigm.

# 2. Related Work and Motivation

A fundamental issue of many previous techniques is the substantial effort required for feature engineering, when dealing with computational graphs. Even if a useful featurization can be found, typically the dependence on rigid aspects of the graph such as connectivity patterns and statistics may not be applicable to similar tasks, making them non-transferrable.

For example, in the compiler and programming languages communities, previous techniques (Akdere et al., 2012; Braberman et al., 2006; Jayakumar et al., 2015; Johnston & Milthorpe, 2018; Nasr-Esfahany et al., 2025) have proposed *count-based* techniques, by counting the occurrences of specific commands or aggregating program metrics and representing their statistics as a final fixed-length vector for tabular regression models such as multi-layer perceptrons (MLPs), random forests, and nearest neighbors. To align more with the graph-based nature of code, other works (Chennupati et al., 2021; Guan & Treude, 2024; Meng & Norris, 2017) first represent code as syntax trees over fixed corpuses of commands and then learn regression model coefficients over either specific components

such as edges, or end-to-end via a GNN. Unfortunately, the moment a new command or kernel is introduced, this may invalidate all previous efforts and the entire process may need to be started from scratch.

Similar design patterns and issues exist for machine learning architectures, especially in field of NAS (Benmeziane et al., 2021; Elsken et al., 2019; White et al., 2023), where a key goal is to predict the performance of trained neural network-based computation graphs. Efforts have consisted of converting such graphs into tabular representations through the use of path encodings (White et al., 2021a), graph statistics (Kadlecová et al., 2024), zero-cost proxies (Abdelfattah et al., 2021) and activation information (Mellor et al., 2021). Other variants include creating graph kernels for the use in Gaussian Processes (Kandasamy et al., 2018; Ru et al., 2021) for Bayesian Optimization, and embeddings via the use of graph neural networks (Akhauri & Abdelfattah, 2024b; Lukasik et al., 2021; Ning et al., 2020; Wen et al., 2020; White et al., 2021b). To extend beyond the scope of purely predicting model accuracy but also latency and cost, additional techniques include hardware embeddings (Akhauri & Abdelfattah, 2024a, 2023; Lee et al., 2021), which require combining different features which have been processed by separate models.

Ideally, the use of minimally structured textual representations can ultimately resolve the issue of feature engineering, by sending strings directly to a single unified text-based regression model. However, such an idea has not yet gained wide popularity, presumably due to questions around their inductive bias, especially for high-precision code and graph regression problems. Nonetheless, there have been attempts (Qin et al., 2025; Zbinden et al., 2022) which attach regression heads to pretrained LLMs for NAS, and other attempts more broadly using LLMs for regression (Lukasik et al., 2025; Vacareanu et al., 2024) over tabular data and recommender systems. Our work crucially differs by establishing the general ability of language models to regress over many different code variants from pure text, which to the best of our knowledge has surprisingly not been investigated, yet is highly valuable for numerous computing fields.

# 3. Method

The RLM method can be taken standard from (Akhauri et al., 2025; Song et al., 2024), which fundamentally treats regression as a simple next-token prediction problem over y-values. The RLM is best structured as an encoder-decoder, which allows input representations of x to be purely in text, taking advantage of the inherent flexibility of strings, and avoiding the need for one-hot representations of categories or normalization of numbers. One distinguishing aspect in this work is the use of a pretrained model (T5Gemma), which we show benefits code regression.

For the decoder side, it is best (as shown in Section 6.4) to use explicit digit-by-digit numeric tokenizations - similar to (Song & Bahri, 2025), we represent y using special sign, exponent, and mantissa tokens, e.g. <+><-><1><7><2><5> represents  $+10^{-1} \times 725 = 72.5$ . This tokenization is also normalization-free, avoiding numeric instabilities or the need to precompute minimum or maximum y-value bounds from data. At inference, constrained decoding is performed to ensure a valid number is always sampled, to either produce a pointwise prediction (via mean or median aggregation of samples) or density estimation with uncertainty quantification (Song & Bahri, 2025).

# 3.1. Multi-task Regression

Due to the universality of both the input and output representations, it is very straightforward to train (x, y) data from multiple different regression tasks, which allows the use of a unified regression model. Furthermore, the RLM allows for a "pretrain then fine-tune" paradigm, where it can be pretrained on

many real or even synthetic regression tasks, and then efficiently few-shot adapt to a new regression task via fine-tuning.

This is especially important as the string-based tokenization opens the doors for use on arbitrary string regression problems, but therefore may require more pretraining (either on regular language data or specific regression tasks) to understand specific structures such as low-level computation graphs better. Contrast this to a hand-crafted and heavily specialized graph regression model which can possess a better inductive bias for such problems, but whose use is restricted to only such formats. This can be more broadly seen as a consequence of the "no-free-lunch" theorem, where more universal methods require more data as they possess a larger space of hypotheses.

# 3.2. Multi-Objective Modeling

Due to the decoder's autoregressive nature, consecutively decoding more numbers also allows conditionally modeling multiple objectives  $p(y' \mid y, x)$  which can naturally capture constraints inherent between different metrics. For example, if the latency (y) of a neural network is too low, the architecture may be too small and thus may not be possible to achieve a certain high level of image classification accuracy (y'). Previous works which rely on parallel regression heads at some embedding vector  $\phi(x)$  are unable to capture correlations between metrics, as they make y and y' conditionally independent with respect to  $\phi(x)$ . We can generalize the conditional modeling to any number of metrics k > 1 via  $p(y^{(k)} \mid y^{(k-1)}, \ldots, y^{(1)}, x)$ , which we show in the experiments can be useful for predicting latencies across multiple hardware platforms.

### 4. Data

# 4.1. High-Level Programming Datasets

We use several high level programming language datasets, to predict either the memory or execution latency from running the program on fixed hardware, as described in Table 1. Here, the texts align better with standard language model pretraining data.

| Dataset    | Samples | Languages | Problem Statement | Input Provided | Latency | Memory |
|------------|---------|-----------|-------------------|----------------|---------|--------|
| CodeNets   | 7.39M   | 37        | ×                 | ×              | ✓       | ✓      |
| APPS       | 98.9K   | 1         | ✓                 | ✓              | ✓       | ✓      |
| KernelBook | 12.6K   | 1         | X                 | $\checkmark$   | ✓       | X      |

Table 1 | Coverage of high-level code datasets.

<u>APPS Leetcode</u>: <u>Hendrycks et al.</u> (2021) contains 10K Python problems, with 232.4K ground-truth solutions and 131.7K test cases. We iterate over the APPS dataset, loading each solution and input-output pair, and run every solution in a minimal sandbox. Our primary metric is peak memory usage. We are able to successfully execute 99K solutions, with further details in Appendix D.4.1.

Triton Kernel Latency: KernelBook (Paliskara & Saroufim, 2025) pairs PyTorch programs with Triton kernels (example: Appendix D.5) produced by TorchInductor. We profile each Triton kernel's latency on a single NVIDIA A6000. Of the 18.2K problems, 12,652 kernels run successfully; most failures stem from our automated argument-matching harness rather than kernel correctness. Further details in Appendix D.4.2.

<u>CodeNet:</u> (Puri et al., 2021) introduces a large-scale dataset consisting of 14M code samples over 37 languages. We filter this dataset by "Accepted" solutions, resulting in 7.3M valid entries across

several languages, and predict over the already provided memory column. Unfortunately, specific input program inputs are not provided, making it impossible to predict the memory *zero-shot* (i.e. new question, new submission). Nonetheless we can still evaluate the RLM on *limited information* scenarios since the train and test splits contain the same set of questions, allowing the RLM to still use few-shot submissions for a question during training, to infer on a submission for the same question at test time.

### 4.2. NAS Datasets

In NAS, the primary objective is to predict the accuracy (e.g. on CIFAR-10) after training a neural network architecture with consistent hyperparameters. In this case our representation of choice is the Open Neural Network Exchange (ONNX) intermediate representation (IR) (ONNX Community, 2017), which contains full information about the auto-differentiation graph used, including all operations used and connectivity patterns. Unique to our work, the ONNX graph representation (example: Appendix D.6) is *universal* as it can represent any neural network or computation graph and is easily transferrable to any new possible neural network. It is also the default representation used in many ML compiler optimization efforts (Kaufman et al., 2021; Phothilimthana et al., 2023; Zheng et al., 2021), opening the doors to domains outside of purely NAS.

| Metric               | Search space |        |        |       |        |        |        |         |       |           |
|----------------------|--------------|--------|--------|-------|--------|--------|--------|---------|-------|-----------|
|                      | NDS          | NB-101 | NB-201 | FBNet | Ofa-MB | Ofa-PN | Ofa-RN | Twopath | Hiaml | Inception |
| Accuracy             | <b>√</b>     | 1      | 1      | Х     | ✓      | ✓      | ✓      | ✓       | ✓     | <b>✓</b>  |
| Latency              | X            | X      | ✓      | ✓     | X      | X      | X      | ×       | X     | X         |
| Architectures        | 44K          | 423K   | 15.6K  | 5K    | 7.5K   | 8.2K   | 10K    | 6.9K    | 4.6K  | 580       |
| <b>Median Tokens</b> | 14K          | 4.1K   | 3.4K   | 3.5K  | 6.3K   | 3.6K   | 2.5K   | 1.8K    | 2.4K  | 23K       |

Table 2 | Coverage of NAS metrics across search spaces.

Summarized in Table 2, we initialize and export all available architectures from NASBench-101 (Ying et al., 2019), NASBench-201 (Dong & Yang, 2020), FBNet (Wu et al., 2019), Once-for-all (Ofa)-MB/PN/RN (Cai et al., 2020), Twopath, Hiaml, Inception (Mills et al., 2023) and Network Design Spaces (NDS) (Radosavovic et al., 2019) to a unified text-based ONNX IR. This amounts to a total of **520K** unique architectures represented in a unified format. We also collate their accuracy, FLOPs, parameter count and latencies. Further, we create our own NAS space (SNAS, see Appendix D.3) of 85.5K architectures, trained on CIFAR-10 for 32 steps, to serve as a pretraining space.

# 5. Experiments

To demonstrate the simplicity of using a unified regressor, we jointly train our model on *all* of the training splits for the datasets mentioned above in Section 4. In Appendix A, we verify that despite absorbing very different forms of regression data (e.g. high-level code and ONNX graphs), the model's performance does not suffer. Appendix C contains exact hyperparameters used.

### 5.1. High-Level Programming Languages

To begin, in Table 3, we find that the RLM produces non-trivial Spearman  $\rho$  performances across multiple programming languages, with the strongest ( $\rho > 0.9$ ) on APPS Leetcode peak-memory. On CodeNet, it performs the best on C++ but also remarkably decently on less common languages such as Lua and Haskell despite using such a small T5Gemma encoder, presumably pretrained minimally on more niche languages.

| Language              | ρ     | Language   | ρ        | Language   | ρ     | Language | ρ     |
|-----------------------|-------|------------|----------|------------|-------|----------|-------|
| C++                   | 0.748 | Go         | 0.670    | Python     | 0.647 | Kotlin   | 0.634 |
| C                     | 0.741 | D          | 0.656    | OCaml      | 0.643 | Swift    | 0.630 |
| Lisp                  | 0.625 | Lua        | 0.618    | Haskell    | 0.611 | Rust     | 0.611 |
| Perl                  | 0.592 | C#         | 0.583    | Java       | 0.560 | Scala    | 0.537 |
| Fortran               | 0.527 | TypeScript | 0.463    | Pascal     | 0.461 | Ruby     | 0.460 |
| Bash                  | 0.455 | F#         | 0.439    | JavaScript | 0.395 | PHP      | 0.347 |
| Triton Kernel Latency |       |            |          |            |       | 0.516    |       |
|                       |       | APPS Le    | etcode I | Memory     |       |          | 0.930 |

Table 3 | Higher ( $\uparrow$ ) is better. Evaluation on all high-level programming datasets, displaying Spearman  $\rho$ . We test 1024 programs per language. For CodeNet, we filter out languages which lack sufficient test examples, leading to 24 languages evaluated.

In Figure 2, we visualize y-values over different tasks and demonstrate the crucial design choice of our normalization-free y-representation, as the model is able to make predictions over a very wide range of scales, from  $10^{-2}$  to  $10^{6}$ .

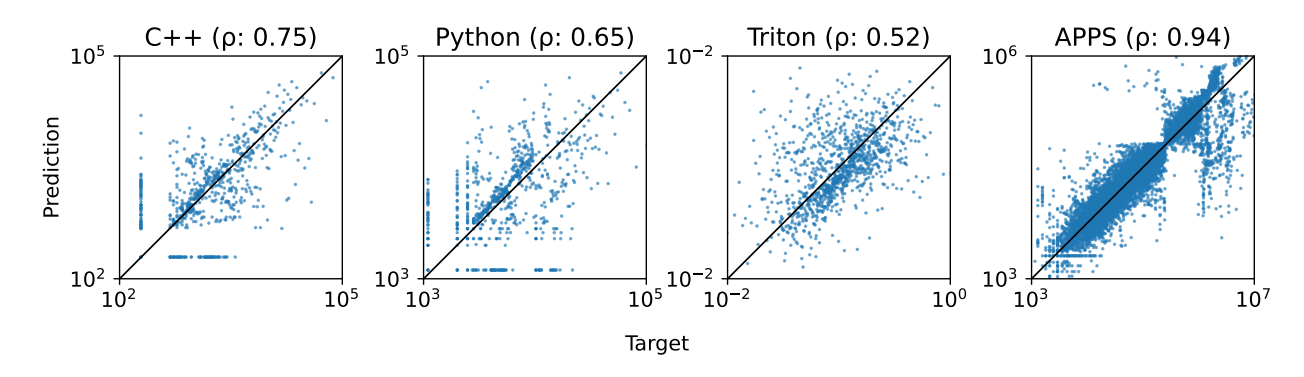


Figure 2 | Diagonal fit ( $\nearrow$ ) is better. Scatterplot of RLM's pointwise y-prediction vs. ground truth value over varying tasks from CodeNet (C++ and Python), Triton Kernels, and APPS. For better visualization, axes are scaled by percentile (probits), and y-value ticks are shown at 10 and 90%.

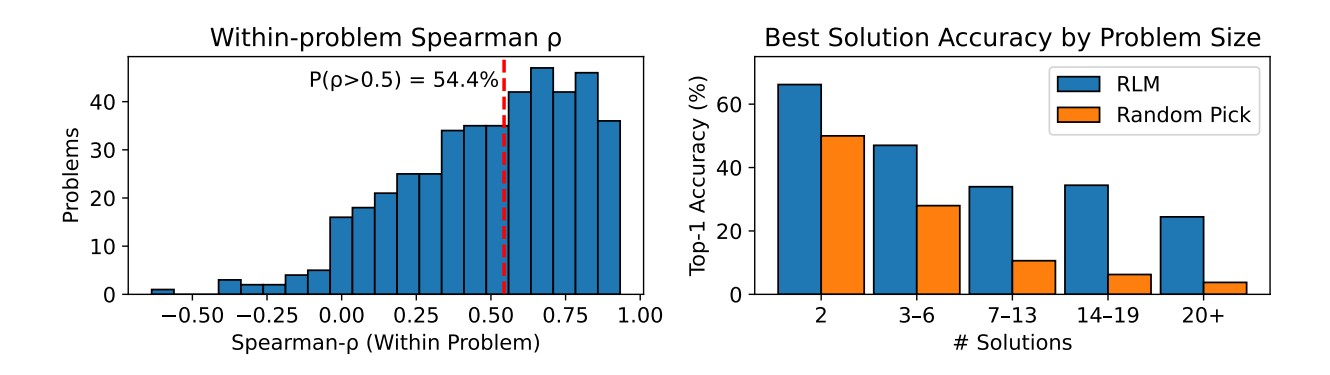


Figure 3 | We identified problems with >8 candidate solution from our test set of 15000, and investigate whether the RLM is able to rank potential solutions. (Left) Distribution of problems and their in-problem Spearman  $\rho$  rankings using the RLM. (Right) RLM vs random selection for choosing the top-1 lowest memory solution from a question, organized by solution count.

Note that one substantial factor negatively influencing Spearman  $\rho$  is the inherent flatness of y-values in some of the data in APPS, independent of the RLM. Using the RLM to rank solutions within a problem, we observed that the 5 problems with the worst performance also possess significantly lower y-value spreads, with median coefficient of variation (CV)  $\approx$  **0.0056** vs **0.037** (7x higher) than the 5 best problems. Furthermore, in Figure 3 (Left), we see that for more than half of problems, the RLM can achieve higher than 0.54 Spearman  $\rho$ , and Figure 3 (Right) and additionally Figure 10 in Appendix B show the RLM can identify the best solution out of multiple submissions to a problem significantly better than random selection.

For qualitative inspection, in Figure 4 and Appendix D.7, we see that the RLM is able to distinguish memory consumption between two substantially different solutions for the same problem.

### Problem (Distance Value)

Given two integer arrays arr1 and arr2, and the integer d, return the distance value between the two arrays. The distance value is defined as the number of elements arr1[i] such that there is not any element arr2[j] where  $|arr1[i] - arr2[j]| \le d$ .

```
Memory-efficient (O(1)) extra space
from typing import List
class Solution:
  def findTheDistanceValue(self, arr1:
    List[int], arr2: List[int], d: int) ->
    # 0(1) memory.
   count = 0
    for a in arr1:
     far = True
      for b in arr2:
        # No allocations
        if abs(a - b) <= d:
          far = False
          # short-circuit
         break
      if far:
       count += 1
    return count
```

```
Less memory-efficient (hash structures)
from typing import List
from collections import Counter
class Solution:
 def findTheDistanceValue(self, arr1:
   List[int], arr2: List[int], d: int) ->
     int:
    # overhead: builds dict
   arr1_counts = Counter(arr1)
    # overhead: build hash set
   arr2set
              = set(arr2)
   for x in arr1_counts:
      target = range(x - d, x + d + 1)
      # overhead: new set
     if arr2set.intersection(target):
        continue
      total += arr1_counts[x]
   return total
```

Figure 4 | Side-by-side solutions from the APPS dataset. Left minimizes memory (O(1) extra space, O(nm) time). Right is often faster due to hash lookups but uses more memory via Counter, set, and per-iteration intersection. RLM predicted **5488** (left) and **10489.5** (right) bytes; ground truth: **5464** and **9672**.

### 5.2. NAS Results

In Figure 4, we further see that the RLM, consuming ONNX strings as input, remains competitive against even SoTA baselines such as FLAN (Akhauri & Abdelfattah, 2024b) and substantially outperforms other graph embedding techniques like Arch2Vec (Yan et al., 2020) which uses a graph autoencoder and CATE (Yan et al., 2021), which encodes architectures by feeding adjacency-matrix–derived token sequences into a Transformer to model global graph structure. We use these encodings with a MLP. Remarkably, the RLM does not require any additional information such as *zero-cost proxies* (Abdelfattah et al., 2021) which are crucial for FLAN to achieve strong results.

In Figure 5, we further demonstrate the RLM's ability for multi-metric prediction, by assessing

| Method                   | NASNet | Amoeba | PNAS  | ENAS  | DARTS | Average |
|--------------------------|--------|--------|-------|-------|-------|---------|
| MLP (Adjacency Enc.)     | 0.002  | 0.032  | 0.082 | 0.021 | 0.124 | 0.052   |
| Arch2Vec (Graph Enc.)    | 0.209  | 0.107  | 0.184 | 0.224 | 0.333 | 0.212   |
| CATE (Transformer Enc.)  | 0.150  | 0.160  | 0.217 | 0.236 | 0.425 | 0.238   |
| GNN                      | 0.364  | 0.376  | 0.444 | 0.438 | 0.523 | 0.429   |
| $FLAN^T$ (Previous SoTA) | 0.344  | 0.470  | 0.430 | 0.484 | 0.567 | 0.459   |
| RLM (Ours)               | 0.382  | 0.488  | 0.427 | 0.481 | 0.528 | 0.461   |

Table 4 | Higher ( $\uparrow$ ) is better. Kendall  $\tau$  rank correlation relative to prior SoTA (FLAN). We use 16 samples from the target search space for NASNet, Amoeba, PNAS and 100 samples for DARTS to match FLAN<sup>T</sup> settings. Note that MLP is trained from scratch due to different adjacency matrix sizes, while we use global representations of Arch2Vec and CATE.

its decoder's ability to produce consecutive metrics. In addition to the accurate predicted Paretofrontier, we also emphasize the slants of the densities, which demonstrate that the RLM decoder has inherently understood the positive correlation between architecture latency and accuracy, a benefit of its autoregressive design.

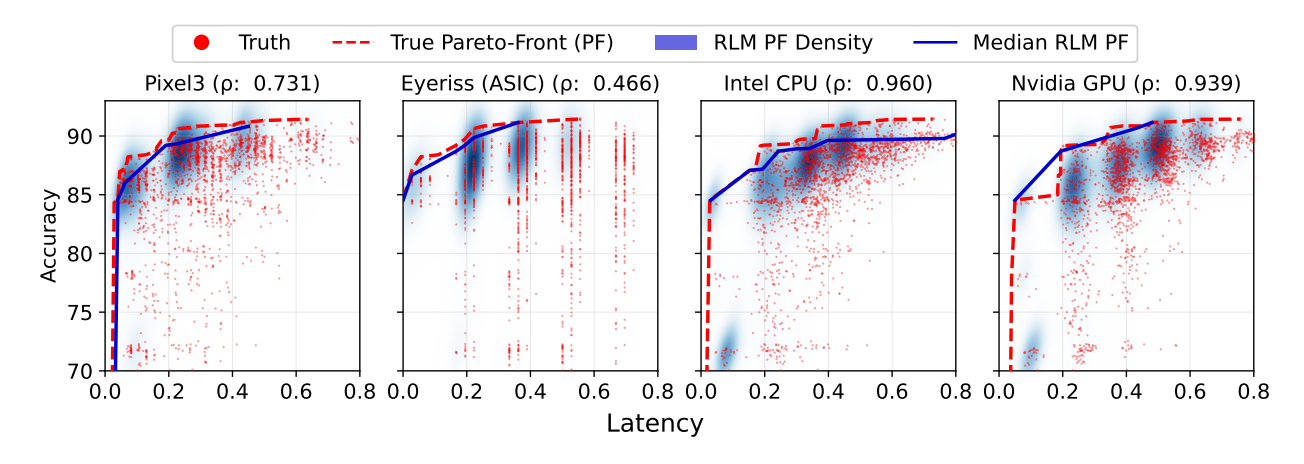


Figure 5 | Single RLM trained on five consecutive objectives on NASBench-201, i.e. first validation accuracy and then hardware-specific latencies over four devices (Pixel3 (Mobile), Eyeriss (ASIC), Intel CPU and Nvidia GPU). Spearman  $\rho$  refers to predicted latency. Density estimates (blue) are plotted for predicted Pareto-optimal points  $x^*$ .

# 6. Experiments: Ablations

# 6.1. Value of Pretraining

We ablate both notions of pretraining, i.e. (1) *language pretraining*: initializing from a (possibly frozen) encoder trained on language data, and (2) *regression pretraining*: initializing from scratch and training purely over (potentially synthetic) regression tasks. Note that these two are not in conflict, as one can still initialize from a language encoder while performing lots of further regression training.

In Figure 6, we see that a language pretrained model trains much better over the Triton Kernel task, leading to lower validation losses and subsequently better regression metrics. Note that freezing the encoder does not impact our run but is significantly cheaper.

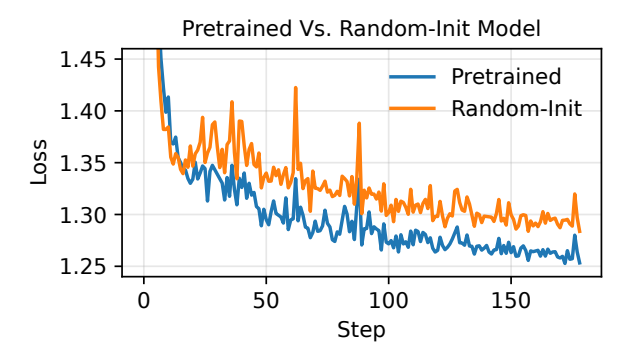


Figure 6 | Lower ( $\downarrow$ ) is better. Validation loss curves when training from T5Gemma checkpoint (0.532  $\rho$ ) vs. random-init (0.504  $\rho$ ).

We further see the complementary value of regression pretraining, especially on cheap synthetic metrics. In Figure 8, we first show that RLMs can learn simple, synthetic metrics nearly perfectly, by pretraining on 381K NASBench-101 samples to predict floating point operations per second (FLOPS) for each architecture. We then reinitialize with this pretrained checkpoint and train over the real task of accuracy prediction from the exact same examples. This accelerates convergence and raises the final Spearman- $\rho$  as well, as shown in Figure 7.

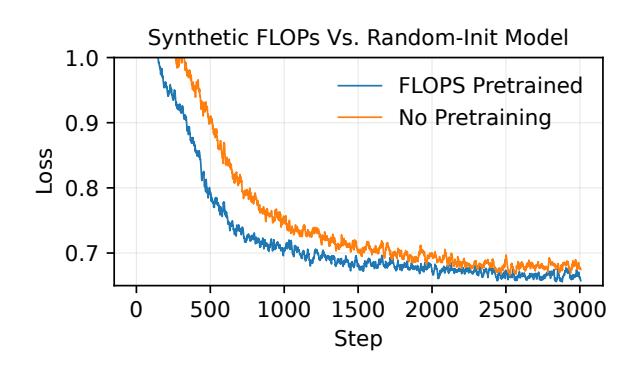


Figure 7 | Lower ( $\downarrow$ ) is better. Validation loss curves when training from synthetic FLOPS pretrained checkpoint (0.85  $\rho$ ) vs. random-init (0.83  $\rho$ ).

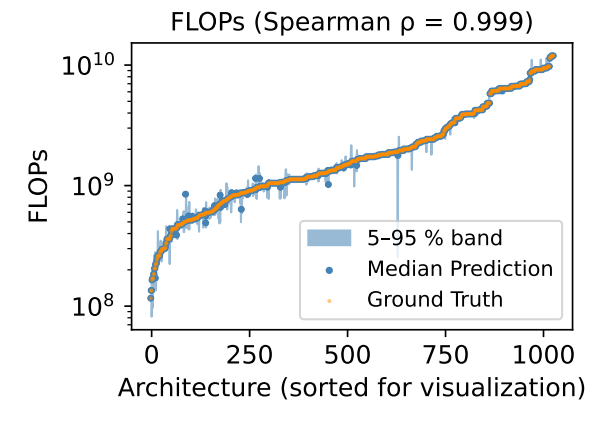


Figure 8 | RLM predictions for FLOPS over 1024 test architectures.

# 6.2. Comparing with Regression Heads

A common misconception is that performing regression with language models requires an explicit regression head (e.g., an MLP on pooled encoder states). To refute this, we use the same number of layers for fairness, and we compare an encoder–decoder (2 layers each) model trained with cross-entropy to an encoder-only (4 layers) model with an explicit regression head trained with mean squared error (MSE). We train these models on three NAS spaces, whose y-value ranges differ markedly (roughly 80–100 for NASBench-101,  $\sim$ 50 for SNAS, and 0–1 for the OFA family).

Since MSE-based heads are sensitive to scale, we therefore evaluate two regression baselines: (i) *Regression Head* (no *y*-normalization) and (ii) *Normalized Regression Head* (*y*-values linearly scaled to [0, 1] per dataset) used by Qin et al. (2025); Zbinden et al. (2022). In Table 5, normalization substantially improves the regression head (Spearman's  $\rho = 0.717$  vs. 0.478 without normalization), yet the decoder head remains best (Spearman's  $\rho = 0.800$ ) and also has the practical advantage of being normalization-free across datasets.

### 6.3. Scaling Regression Language Models

Akhauri et al. (2025) previously found that models trained from scratch, produce lower validation losses with increased parameter counts (up to 250M). To demonstrate scaling via pretrained models, we also train a 600M parameter model (HuggingFace: t5gemma-b-b-prefixlm) using the exact same settings as our default 300M model, and verify that it performs better (Table 6). However, we

| Head                       | Spearman-ρ |
|----------------------------|------------|
| Regression Head            | 0.478      |
| Normalized Regression Head | 0.717      |
| Decoder Head (Ours)        | 0.800      |

| Table 5   Higher (↑) is better. Evaluations on 512 |
|--|
| NASBench-101 test examples, using models pre-      |
| trained on a subset of NASBench-101, SNAS, OfaRN,  |
| OfaPN, and OfaMB.                                  |

| T5Gemma      | Params | Spearman-ρ |
|--------------|--------|------------|
| s-s-prefixlm | 300M   | 0.744      |
| b-b-prefixlm | 600M   | 0.782      |

Table 6 | Higher (↑) is better. Evaluations on 1024 CodeNet examples, using RLMs with different pretrained T5Gemma encoder sizes, trained on a smaller subset of CodeNet, APPS and KernelBook.

found that larger models in the T5Gemma family require extensive hyperparameter tuning and could not be run under limited compute - we leave further scaling analysis for future work.

### 6.4. Encoder-Decoder Settings

Custom Encoder Tokenizations: We train an encoder-decoder from scratch and using SentencePiece (Kudo & Richardson, 2018) tokenization, compare using T5's default (32K tokens) (Raffel et al., 2020) to a custom, compact ONNX-aware tokenizer (8K tokens) learned from plain-text ONNX dumps. The learned tokenizer merges frequent operator strings (e.g., MaxPool) and reduces token counts, allowing longer graphs per sequence. This leads to a marked improvement in Table 7.

|                 | T5 (32K) | Learned (8K) |  |
|-----------------|----------|--------------|--|
| Spearman- $ ho$ | 0.533    | 0.723        |  |

|     | 1K    | 2K    | 4K    |
|-----|-------|-------|-------|
| RLM | 0.819 | 0.833 | 0.838 |

enizers and training on 381K NASBench-101 examples 381K NASBench-101 examples, for two epochs. for one epoch.

Table 7 | Higher ( $\uparrow$ ) is better. Spearman rank on 1024 Table 8 | Higher ( $\uparrow$ ) is better. Sequence length ablatest examples, when using default T5 vs. learned tok- tion (Spearman- $\rho$ ) using learned encoder tokenizer on

Longer Sequence Lengths: Using the learned tokenizer, increasing the encoder context allows the RLM to read more information about the graph, and thus improves rank correlation when using the same training procedure, with Spearman- $\rho$  rising from 0.819 (1K) to 0.838 (4K) in Table 8.

Decoder Tokenization and Initialization: The only change to the regular T5Gemma design is our use of our explicit digit-by-digit custom numeric tokenization with constrained decoding. To understand its effects, in Table 9, we see the digitby-digit tokenizer leads to better results against the regular T5Gemma tokenizer (i.e. 72.5 literally represented as 72.5), as it induces better structuring on numbers and significantly simplifies decode token choices. Furthermore, using the pretrained T5Gemma decoder only helps

| Tokenization                     | Decoder I<br>Random | nitialization<br>Pretrained |
|----------------------------------|---------------------|-----------------------------|
| Explicit Digit (Ours)<br>T5Gemma | <b>0.747</b> 0.654  | <b>0.744</b> 0.698          |

Table 9 | Higher is better (†). Evaluation on 1024 CodeNet samples after training. Note: Explicit digit tokenizer with pretrained decoder required resetting token embedding tables and final logit projection layer.

the T5Gemma tokenizer, presumably from relevant knowledge of numbers in common text format. However, digit-by-digit tokenizer performance remains unchanged regardless of decoder pretraining, implying that only the T5Gemma pretrained encoder suffices for use.

# 7. Conclusion

Aligned with the standard generative pretraining paradigm (Radford et al., 2018), we have shown that RLMs are effective regression models for many types of programming languages and code representations, without requiring any post-processing or feature engineering of raw data. Applications include speeding up program search (Li et al., 2022; Real et al., 2020; Romera-Paredes et al., 2024), hardware-software co-design (Micheli & Gupta, 1997; Patterson & Hennessy, 2013), and compiler optimization (Ashouri et al., 2018; Wang & O'Boyle, 2018). A key open question is whether such code-based RLMs can be more broadly used to predict the numeric outcome of entire experiments from raw code, but we leave this to future work and hope this paper will be a valuable reference for multiple scientific communities in automated machine learning, programming languages, and computer architecture.

# Acknowledgements

We would like to thank Amir Yazdanbakhsh for providing feedback on initial drafts of this paper, and Quoc Le, Chen Liang, Dara Bahri, Cheng-Hsi Lin, Bangding Yang, Jiyoun Ha, Jonathan Lai, Fred Zhang, and Yangsibo Huang for useful discussions.

# References

- Mohamed S. Abdelfattah, Abhinav Mehrotra, Lukasz Dudziak, and Nicholas Donald Lane. Zero-cost proxies for lightweight NAS. In 9th International Conference on Learning Representations, ICLR 2021, Virtual Event, Austria, May 3-7, 2021, 2021.
- Mert Akdere, Ugur Çetintemel, Matteo Riondato, Eli Upfal, and Stanley B. Zdonik. Learning-based query performance modeling and prediction. In Anastasios Kementsietsidis and Marcos Antonio Vaz Salles (eds.), *IEEE 28th International Conference on Data Engineering (ICDE 2012), Washington, DC, USA (Arlington, Virginia), 1-5 April, 2012*, pp. 390–401. IEEE Computer Society, 2012. doi: 10.1109/ICDE.2012.64.
- Yash Akhauri and Mohamed Abdelfattah. On latency predictors for neural architecture search. *Proceedings of Machine Learning and Systems*, 6:512–523, 2024a.
- Yash Akhauri and Mohamed S. Abdelfattah. Multi-predict: Few shot predictors for efficient neural architecture search. In Aleksandra Faust, Roman Garnett, Colin White, Frank Hutter, and Jacob R. Gardner (eds.), *International Conference on Automated Machine Learning*, 12-15 November 2023, Hasso Plattner Institute, Potsdam, Germany, volume 224 of Proceedings of Machine Learning Research, pp. 23/1–23. PMLR, 2023.
- Yash Akhauri and Mohamed S. Abdelfattah. Encodings for prediction-based neural architecture search. In Forty-first International Conference on Machine Learning, ICML 2024, Vienna, Austria, July 21-27, 2024, 2024b.
- Yash Akhauri, Bryan Lewandowski, Cheng-Hsi Lin, Adrian N. Reyes, Grant C. Forbes, Arissa Wongpanich, Bangding Yang, Mohamed S. Abdelfattah, Sagi Perel, and Xingyou Song. Performance prediction for large systems via text-to-text regression. *arXiv preprint arXiv:2506.21718*, 2025.
- Amir H. Ashouri, Josep L. Berral, Grigori Fursin, Sylvain Girbal, Sergei Gorlatch, Bastian Hagedorn, Michael Haidl, Ho-Chun Ho, Hsiang-Tsung Hsiao, Sameer Kulkarni, et al. A survey on compiler autotuning using machine learning. *ACM Computing Surveys (CSUR)*, 51(5), 2018. doi: 10.1145/3197978.
- Hadjer Benmeziane, Kaoutar El Maghraoui, Hamza Ouarnoughi, Smail Niar, Martin Wistuba, and Naigang Wang. Hardware-aware neural architecture search: Survey and taxonomy. In Zhi-Hua Zhou (ed.), *Proceedings of the Thirtieth International Joint Conference on Artificial Intelligence, IJCAI-21*, pp. 4322–4329. International Joint Conferences on Artificial Intelligence Organization, 8 2021. doi: 10.24963/ijcai.2021/592. Survey Track.
- Jon Bentley. Programming pearls: Algorithm design techniques. *Communications of the ACM*, 27(9): 865–873, 1984. doi: 10.1145/358234.381162.
- Víctor Braberman, Diego Garbervetsky, and Sergio Yovine. A static analysis for synthesizing parametric specifications of dynamic memory consumption. *Journal of Object Technology*, 5(5):31–58, June 2006.
- Han Cai, Chuang Gan, Tianzhe Wang, Zhekai Zhang, and Song Han. Once for all: Train one network and specialize it for efficient deployment. In *International Conference on Learning Representations*, 2020.
- Gopinath Chennupati, Nandakishore Santhi, Phill Romero, and Stephan Eidenbenz. Machine learning–enabled scalable performance prediction of scientific codes. *ACM Trans. Model. Comput. Simul.*, 31(2), April 2021. ISSN 1049-3301. doi: 10.1145/3450264.

- Xuanyi Dong and Yi Yang. Nas-bench-201: Extending the scope of reproducible neural architecture search. In 8th International Conference on Learning Representations, ICLR 2020, Addis Ababa, Ethiopia, April 26-30, 2020, 2020.
- Thomas Elsken, Jan Hendrik Metzen, and Frank Hutter. Neural architecture search: a survey. *J. Mach. Learn. Res.*, 20(1):1997–2017, January 2019. ISSN 1532-4435.
- Xueting Guan and Christoph Treude. Enhancing source code representations for deep learning with static analysis. In Igor Steinmacher, Mario Linares-Vásquez, Kevin Patrick Moran, and Olga Baysal (eds.), *Proceedings of the 32nd IEEE/ACM International Conference on Program Comprehension, ICPC 2024, Lisbon, Portugal, April 15-16, 2024*, pp. 64–68. ACM, 2024. doi: 10.1145/3643916.3644396.
- Dan Hendrycks, Steven Basart, Saurav Kadavath, Mantas Mazeika, Akul Arora, Ethan Guo, Collin Burns, Samir Puranik, Horace He, Dawn Song, and Jacob Steinhardt. Measuring coding challenge competence with apps. *NeurIPS*, 2021.
- Dong Huang, Yuhao Qing, Weiyi Shang, Heming Cui, and Jie M. Zhang. Effibench: benchmarking the efficiency of automatically generated code. In *Proceedings of the 38th International Conference on Neural Information Processing Systems*, NIPS '24, Red Hook, NY, USA, 2025. Curran Associates Inc. ISBN 9798331314385.
- Anirudh Jayakumar, Prakash Murali, and Sathish Vadhiyar. Matching application signatures for performance predictions using a single execution. In *2015 IEEE International Parallel and Distributed Processing Symposium*, pp. 1161–1170, 2015. doi: 10.1109/IPDPS.2015.20.
- Beau Johnston and Josh Milthorpe. Aiwc: Opencl-based architecture-independent workload characterization. In *2018 IEEE/ACM 5th Workshop on the LLVM Compiler Infrastructure in HPC (LLVM-HPC)*, pp. 81–91, 2018. doi: 10.1109/LLVM-HPC.2018.8639381.
- Gabriela Kadlecová, Jovita Lukasik, Martin Pilát, Petra Vidnerová, Mahmoud Safari, Roman Neruda, and Frank Hutter. Surprisingly strong performance prediction with neural graph features. In Forty-first International Conference on Machine Learning, ICML 2024, Vienna, Austria, July 21-27, 2024, 2024.
- Kirthevasan Kandasamy, Willie Neiswanger, Jeff Schneider, Barnabás Póczos, and Eric P. Xing. Neural architecture search with bayesian optimisation and optimal transport. In *Proceedings of the 32nd International Conference on Neural Information Processing Systems*, NIPS'18, pp. 2020–2029, Red Hook, NY, USA, 2018. Curran Associates Inc.
- Samuel J. Kaufman, Phitchaya Mangpo Phothilimthana, Yanqi Zhou, Charith Mendis, Sudip Roy, Amit Sabne, and Mike Burrows. A learned performance model for tensor processing units. In Alex Smola, Alex Dimakis, and Ion Stoica (eds.), *Proceedings of the Fourth Conference on Machine Learning and Systems, MLSys 2021, virtual, April 5-9, 2021.* mlsys.org, 2021.
- Taku Kudo and John Richardson. Sentencepiece: A simple and language independent subword tokenizer and detokenizer for neural text processing. In *Proceedings of the 2018 Conference on Empirical Methods in Natural Language Processing: System Demonstrations*, pp. 66–71, 2018.
- Hayeon Lee, Sewoong Lee, Song Chong, and Sung Ju Hwang. Hardware-adaptive efficient latency prediction for NAS via meta-learning. In Marc'Aurelio Ranzato, Alina Beygelzimer, Yann N. Dauphin, Percy Liang, and Jennifer Wortman Vaughan (eds.), *Advances in Neural Information Processing Systems 34: Annual Conference on Neural Information Processing Systems 2021, NeurIPS 2021, December 6-14, 2021, virtual*, pp. 27016–27028, 2021.

- Yujia Li, David Choi, Junyoung Chung, Nate Kushman, Julian Schrittwieser, Rémi Leblond, Tom Eccles, James Keeling, Felix Gimeno, Agustin Dal Lago, Thomas Hubert, Peter Choy, Cyprien de Masson d'Autume, Igor Babuschkin, Xinyun Chen, Po-Sen Huang, Johannes Welbl, Sven Gowal, Alexey Cherepanov, James Molloy, Daniel J. Mankowitz, Esme Sutherland Robson, Pushmeet Kohli, Nando de Freitas, Koray Kavukcuoglu, and Oriol Vinyals. Competition-level code generation with alphacode. Science, 378(6624):1092–1097, 2022. doi: 10.1126/science.abq1158.
- Jovita Lukasik, David Friede, Arber Zela, Frank Hutter, and Margret Keuper. Smooth variational graph embeddings for efficient neural architecture search. In *International Joint Conference on Neural Networks, IJCNN 2021, Shenzhen, China, July 18-22, 2021*, pp. 1–8. IEEE, 2021. doi: 10.1109/IJCNN52387.2021.9534092.
- Michal Lukasik, Zhao Meng, Harikrishna Narasimhan, Aditya Krishna Menon, Yin Wen Chang, Felix X. Yu, and Sanjiv Kumar. Better autoregressive regression with LLMs. In *The Thirteenth International Conference on Learning Representations, ICLR 2025, Singapore, Singapore, April 24-28, 2025*. OpenReview.net, 2025.
- Joe Mellor, Jack Turner, Amos J. Storkey, and Elliot J. Crowley. Neural architecture search without training. In Marina Meila and Tong Zhang (eds.), *Proceedings of the 38th International Conference on Machine Learning, ICML 2021, 18-24 July 2021, Virtual Event*, volume 139 of *Proceedings of Machine Learning Research*, pp. 7588–7598. PMLR, 2021.
- Kewen Meng and Boyana Norris. Mira: A framework for static performance analysis. In *2017 IEEE International Conference on Cluster Computing (CLUSTER)*, pp. 103–113, 2017. doi: 10.1109/CLUSTER.2017.43.
- G. De Micheli and R. K. Gupta. Hardware/software co-design. *Proceedings of the IEEE*, 85(3):349–365, 1997. doi: 10.1109/5.558708.
- Keith G. Mills, Fred X. Han, Jialin Zhang, Fabian Chudak, Ali Safari Mamaghani, Mohammad Salameh, Wei Lu, Shangling Jui, and Di Niu. GENNAPE: towards generalized neural architecture performance estimators. In Brian Williams, Yiling Chen, and Jennifer Neville (eds.), *Thirty-Seventh AAAI Conference on Artificial Intelligence, AAAI 2023, Thirty-Fifth Conference on Innovative Applications of Artificial Intelligence, IAAI 2023, Thirteenth Symposium on Educational Advances in Artificial Intelligence, EAAI 2023, Washington, DC, USA, February 7-14, 2023*, pp. 9190–9199. AAAI Press, 2023. doi: 10.1609/AAAI.V37I8.26102.
- Arash Nasr-Esfahany, Mohammad Alizadeh, Victor Lee, Hanna Alam, Brett W. Coon, David E. Culler, Vidushi Dadu, Martin Dixon, Henry M. Levy, Santosh Pandey, Parthasarathy Ranganathan, and Amir Yazdanbakhsh. Concorde: Fast and accurate CPU performance modeling with compositional analytical-ml fusion. In *Proceedings of the 52nd Annual International Symposium on Computer Architecture, ISCA 2025, Tokyo, Japan, June 21-25, 2025*, pp. 1480–1494. ACM, 2025. doi: 10.1145/3695053.3731037.
- Xuefei Ning, Yin Zheng, Tianchen Zhao, Yu Wang, and Huazhong Yang. A generic graph-based neural architecture encoding scheme for predictor-based NAS. In Andrea Vedaldi, Horst Bischof, Thomas Brox, and Jan-Michael Frahm (eds.), Computer Vision ECCV 2020 16th European Conference, Glasgow, UK, August 23-28, 2020, Proceedings, Part XIII, volume 12358 of Lecture Notes in Computer Science, pp. 189–204. Springer, 2020. doi: 10.1007/978-3-030-58601-0\\_12.
- ONNX Community. Open neural network exchange (onnx). https://onnx.ai/, 2017.
- Sahan Paliskara and Mark Saroufim. Kernelbook, 5 2025. URL https://huggingface.co/datasets/GPUMODE/KernelBook.

- David A. Patterson and John L. Hennessy. *Computer Organization and Design: The Hardware/Software Interface*. Morgan Kaufmann, 5th edition, 2013.
- Phitchaya Mangpo Phothilimthana, Sami Abu-El-Haija, Kaidi Cao, Bahare Fatemi, Michael Burrows, Charith Mendis, and Bryan Perozzi. Tpugraphs: A performance prediction dataset on large tensor computational graphs. In Alice Oh, Tristan Naumann, Amir Globerson, Kate Saenko, Moritz Hardt, and Sergey Levine (eds.), Advances in Neural Information Processing Systems 36: Annual Conference on Neural Information Processing Systems 2023, NeurIPS 2023, New Orleans, LA, USA, December 10-16, 2023, 2023.
- Ruchir Puri, David S Kung, Geert Janssen, Wei Zhang, Giacomo Domeniconi, Vladimir Zolotov, Julian Dolby, Jie Chen, Mihir Choudhury, Lindsey Decker, et al. Codenet: A large-scale ai for code dataset for learning a diversity of coding tasks. *arXiv preprint arXiv:2105.12655*, 2021.
- Shiwen Qin, Gabriela Kadlecová, Martin Pilát, Shay B Cohen, Roman Neruda, Elliot J. Crowley, Jovita Lukasik, and Linus Ericsson. Transferrable surrogates in expressive neural architecture search spaces. In *AutoML 2025 Methods Track*, 2025.
- Alec Radford, Karthik Narasimhan, Tim Salimans, and Ilya Sutskever. Improving language understanding by generative pre-training. Technical report, OpenAI, 2018. Technical Report.
- Ilija Radosavovic, Justin Johnson, Saining Xie, Wan-Yen Lo, and Piotr Dollár. On network design spaces for visual recognition. In 2019 IEEE/CVF International Conference on Computer Vision, ICCV 2019, Seoul, Korea (South), October 27 November 2, 2019, pp. 1882–1890. IEEE, 2019. doi: 10.1109/ICCV.2019.00197.
- Colin Raffel, Noam Shazeer, Adam Roberts, Katherine Lee, Sharan Narang, Michael Matena, Yanqi Zhou, Wei Li, and Peter J. Liu. Exploring the limits of transfer learning with a unified text-to-text transformer. *J. Mach. Learn. Res.*, 21:140:1–140:67, 2020.
- Esteban Real, Chen Liang, David R. So, and Quoc V. Le. Automl-zero: Evolving machine learning algorithms from scratch. In *Proceedings of the 37th International Conference on Machine Learning, ICML 2020, 13-18 July 2020, Virtual Event*, volume 119 of *Proceedings of Machine Learning Research*, pp. 8007–8019. PMLR, 2020. URL http://proceedings.mlr.press/v119/real20a.html.
- Bernardino Romera-Paredes, Mohammadamin Barekatain, Alexander Novikov, Matej Balog, M. Pawan Kumar, Emilien Dupont, Francisco J. R. Ruiz, Jordan S. Ellenberg, Pengming Wang, Omar Fawzi, Pushmeet Kohli, and Alhussein Fawzi. Mathematical discoveries from program search with large language models. *Nat.*, 625(7995):468–475, 2024. doi: 10.1038/S41586-023-06924-6.
- Bin Xin Ru, Xingchen Wan, Xiaowen Dong, and Michael A. Osborne. Interpretable neural architecture search via bayesian optimisation with weisfeiler-lehman kernels. In *9th International Conference on Learning Representations, ICLR 2021, Virtual Event, Austria, May 3-7, 2021*, 2021.
- Xingyou Song and Dara Bahri. Decoding-based regression. *Transactions on Machine Learning Research*, 2025. ISSN 2835-8856.
- Xingyou Song, Oscar Li, Chansoo Lee, Bangding Yang, Daiyi Peng, Sagi Perel, and Yutian Chen. Omnipred: Language models as universal regressors. *Trans. Mach. Learn. Res.*, 2024.
- Robert Vacareanu, Vlad-Andrei Negru, Vasile Suciu, and Mihai Surdeanu. From words to numbers: Your large language model is secretly A capable regressor when given in-context examples. *CoRR*, abs/2404.07544, 2024.

- Zheng Wang and Michael F. P. O'Boyle. Machine learning in compiler optimisation. *Proceedings of the IEEE*, 106(11):1879–1901, 2018. doi: 10.1109/JPROC.2018.2838688.
- Wei Wen, Hanxiao Liu, Yiran Chen, Hai Li, Gabriel Bender, and Pieter-Jan Kindermans. Neural predictor for neural architecture search. In Andrea Vedaldi, Horst Bischof, Thomas Brox, and Jan-Michael Frahm (eds.), *Computer Vision ECCV 2020*, pp. 660–676, Cham, 2020. Springer International Publishing. ISBN 978-3-030-58526-6.
- Colin White, Willie Neiswanger, and Yash Savani. BANANAS: bayesian optimization with neural architectures for neural architecture search. In *Thirty-Fifth AAAI Conference on Artificial Intelligence, AAAI 2021, Thirty-Third Conference on Innovative Applications of Artificial Intelligence, IAAI 2021, The Eleventh Symposium on Educational Advances in Artificial Intelligence, EAAI 2021, Virtual Event, February 2-9, 2021*, pp. 10293–10301. AAAI Press, 2021a. doi: 10.1609/AAAI.V35I12.17233.
- Colin White, Arber Zela, Robin Ru, Yang Liu, and Frank Hutter. How powerful are performance predictors in neural architecture search? In Marc'Aurelio Ranzato, Alina Beygelzimer, Yann N. Dauphin, Percy Liang, and Jennifer Wortman Vaughan (eds.), *Advances in Neural Information Processing Systems 34*: Annual Conference on Neural Information Processing Systems 2021, NeurIPS 2021, December 6-14, 2021, virtual, pp. 28454–28469, 2021b.
- Colin White, Mahmoud Safari, Rhea Sukthanker, Binxin Ru, Thomas Elsken, Arber Zela, Debadeepta Dey, and Frank Hutter. Neural architecture search: Insights from 1000 papers. *CoRR*, abs/2301.08727, 2023. doi: 10.48550/ARXIV.2301.08727.
- Bichen Wu, Xiaoliang Dai, Peizhao Zhang, Yanghan Wang, Fei Sun, Yiming Wu, Yuandong Tian, Peter Vajda, Yangqing Jia, and Kurt Keutzer. Fbnet: Hardware-aware efficient convnet design via differentiable neural architecture search. In *IEEE Conference on Computer Vision and Pattern Recognition, CVPR 2019, Long Beach, CA, USA, June 16-20, 2019*, pp. 10734–10742. Computer Vision Foundation / IEEE, 2019. doi: 10.1109/CVPR.2019.01099.
- Shen Yan, Yu Zheng, Wei Ao, Xiao Zeng, and Mi Zhang. Does unsupervised architecture representation learning help neural architecture search? In Hugo Larochelle, Marc'Aurelio Ranzato, Raia Hadsell, Maria-Florina Balcan, and Hsuan-Tien Lin (eds.), *Advances in Neural Information Processing Systems* 33: Annual Conference on Neural Information Processing Systems 2020, NeurIPS 2020, December 6-12, 2020, virtual, 2020.
- Shen Yan, Kaiqiang Song, Fei Liu, and Mi Zhang. CATE: computation-aware neural architecture encoding with transformers. In Marina Meila and Tong Zhang (eds.), *Proceedings of the 38th International Conference on Machine Learning, ICML 2021, 18-24 July 2021, Virtual Event*, volume 139 of *Proceedings of Machine Learning Research*, pp. 11670–11681. PMLR, 2021.
- Chris Ying, Aaron Klein, Eric Christiansen, Esteban Real, Kevin Murphy, and Frank Hutter. Nasbench-101: Towards reproducible neural architecture search. In Kamalika Chaudhuri and Ruslan Salakhutdinov (eds.), *Proceedings of the 36th International Conference on Machine Learning, ICML 2019, 9-15 June 2019, Long Beach, California, USA*, volume 97 of *Proceedings of Machine Learning Research*, pp. 7105–7114. PMLR, 2019.
- Robin Zbinden, Lukas Mauch, and Fabien Cardinaux. COBRA: Enhancing DNN latency prediction with language models trained on source code. In *Deep Learning for Code Workshop*, 2022.
- Lianmin Zheng, Ruochen Liu, Junru Shao, Tianqi Chen, Joseph Gonzalez, Ion Stoica, and Ameer Haj-Ali. Tenset: A large-scale program performance dataset for learned tensor compilers. In Joaquin Vanschoren and Sai-Kit Yeung (eds.), *Proceedings of the Neural Information Processing Systems Track*

| on Datasets and Benchmarks 1, 2021. | NeurIPS Datasets and | Benchmarks 2021, | December 202 | 1, virtual, |
|-------------------------------------|----------------------|------------------|--------------|-------------|
|                                     |                      |                  |              |             |
|                                     |                      |                  |              |             |
|                                     |                      |                  |              |             |
|                                     |                      |                  |              |             |
|                                     |                      |                  |              |             |
|                                     |                      |                  |              |             |
|                                     |                      |                  |              |             |
|                                     |                      |                  |              |             |
|                                     |                      |                  |              |             |
|                                     |                      |                  |              |             |
|                                     |                      |                  |              |             |
|                                     |                      |                  |              |             |
|                                     |                      |                  |              |             |
|                                     |                      |                  |              |             |
|                                     |                      |                  |              |             |
|                                     |                      |                  |              |             |
|                                     |                      |                  |              |             |

### A. Unified Model Ablations

# A.1. Training on Code and NAS

We verify below that training a unified model on both code and graphs does not harm its performance. In Table 10, a model trained with additional NAS graph data does *not* negatively impact ranking effectiveness (up to statistical significance) on any of the coding benchmarks, demonstrating that the RLM is able to absorb different domains.

| Pretrain Corpus | APPS (Py) | CN (C) | CN (C++) | CN (Py) | KernelBook | Avg.  |
|-----------------|-----------|--------|----------|---------|------------|-------|
| Code            | 0.942     | 0.684  | 0.741    | 0.651   | 0.486      | 0.701 |
| Code + Graphs   | 0.925     | 0.740  | 0.733    | 0.634   | 0.499      | 0.706 |

Table 10 | Higher ( $\uparrow$ ) is better. Spearman's  $\rho$  values for an RLM trained only on code vs. an RLM trained additionally on NAS, when tested on coding benchmarks. We test on 1024 examples per language. CodeNet abbreviated as CN.

In Figure 9, we also see that throughout the training process, the validation Spearman  $\rho$  does not change either, demonstrating consistent performance regardless of convergence.

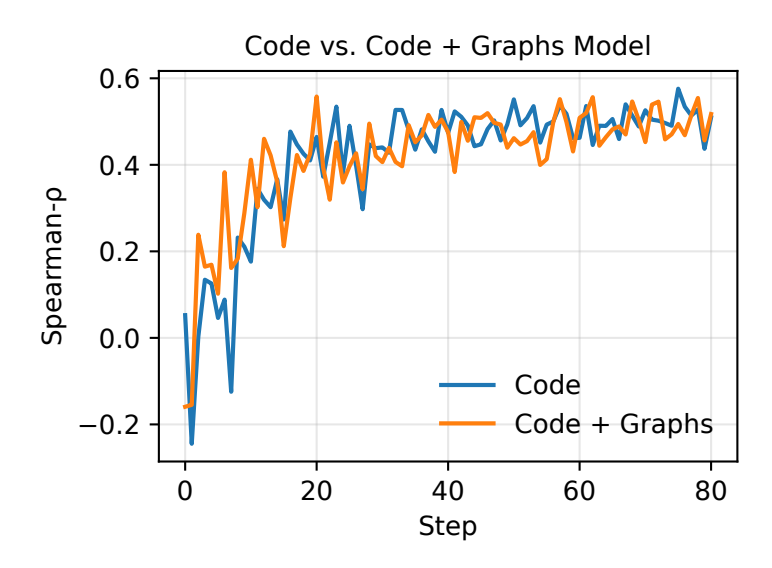


Figure 9 | Higher is better ( $\uparrow$ ). Spearman  $\rho$  on KernelBook examples, over different training checkpoints.

# A.2. Pretraining Diversity and Impact on Language

One important question is whether training on one language helps evaluation on other languages, as there may be some overlap in syntax or general programming styles. To study this using CodeNet, we fix the evaluation to always be over three languages (Go, Haskell, and Rust) while varying the pretraining mixture.

To remain fair, all models are trained over 482K examples, which always contains 45K fixed examples (15K from each language to be evaluated). The rest of the 437K examples are varied:

• One Language: C++ (437K samples)

- Two Languages: C++, Python (218.7K each)
- Four Languages: C++, Python, Java, Ruby (109.4K each)
- Six Languages: C++, Python, Java, Ruby, C#, C (72.9K each)

|           | In   | -Distributi | on   |      | Purely Zero-Shot |            |        |       |      |      |       |         |
|-----------|------|-------------|------|------|------------------|------------|--------|-------|------|------|-------|---------|
| Languages | Go   | Haskell     | Rust | D    | Fortran          | JavaScript | Kotlin | OCaml | PHP  | Perl | Scala | Average |
| One       | 0.61 | 0.56        | 0.57 | 0.53 | 0.38             | 0.29       | 0.49   | 0.58  | 0.33 | 0.23 | 0.40  | 0.45    |
| Two       | 0.62 | 0.57        | 0.57 | 0.56 | 0.30             | 0.34       | 0.54   | 0.60  | 0.24 | 0.17 | 0.40  | 0.45    |
| Four      | 0.61 | 0.51        | 0.56 | 0.55 | 0.28             | 0.25       | 0.39   | 0.52  | 0.12 | 0.05 | 0.25  | 0.37    |
| Six       | 0.61 | 0.54        | 0.55 | 0.52 | 0.34             | 0.31       | 0.44   | 0.57  | 0.27 | 0.17 | 0.37  | 0.43    |

Table 11 | Higher ( $\uparrow$ ) is better. Spearman  $\rho$  results across languages.

As shown in Table 11, increasing the number of pretraining languages does not clearly improve performance on unseen languages. For the three evaluation languages, the results stay roughly the same across all settings. For purely zero-shot languages that the model never saw during training (e.g. D, Fortran, ...), the increased pretraining diversity even sometimes leads to worse results.

We hypothesize this occurs because of the structure of the CodeNet dataset, which contains 13,916,868 submissions divided across 4053 problems. In practice, seeing more diverse problems in a single language may be more helpful than seeing the same problems repeated across multiple languages. In other words, the model benefits more from variety in problem content than from variety in programming syntax. This effect may be reinforced by the strong T5Gemma encoder, which already encodes different programming languages well, making additional cross-language diversity less important.

### A.3. Fine-tuning

In Table 12, we further show that even fine-tuning on data from a specific language, does *not* necessarily help its performance when the task was already richly observed from the pretraining corpus. We hypothesize this is a form of "catastrophic forgetting", where over-focusing on a specific language can actually negatively affect general reasoning and regression abilities, driving the overall result down. Furthermore, T5Gemma encoder is already well-calibrated for code, and thus the benefit of fine-tuning with just 1024 samples may be relatively limited.

| C++ | С | Go | Python | Rust | Haskell        | C# | Java | Ruby | Triton |
|-----|---|----|--------|------|----------------|----|------|------|--------|
|     |   |    |        |      | 0.577<br>0.546 |    |      |      |        |

Table 12 | Higher ( $\uparrow$ ) is better. Spearman  $\rho$  performance of models with and without fine-tuning (FT) across different programming languages. The model is pretrained on a sufficiently large corpus of code, and does not benefit from 1024 new few-shot examples specific to the language being evaluated. We test 1024 programs per language.

For NAS however, fine-tuning *does* benefit performance on out-of-domain tasks. In Table 13, we took our pretrained model on both code and NAS, and fine-tune it an an additional 1K samples from the target NAS search space. While Amoeba and ENAS were in the pretraining set, they were only 0.08% of the pretraining corpus, while the total NAS data also only occupied 1.1%. Thus for such low-resource tasks, there is significant benefit to fine-tuning the RLM, leading to the massive gains (+0.35 Spearman  $\rho$  on Amoeba and ENAS).

|       | NASBench201 | NASBench101 | ENAS  | Amoeba |
|-------|-------------|-------------|-------|--------|
| No FT | 0.681       | 0.646       | 0.165 | 0.045  |
| FT    | 0.738       | 0.734       | 0.516 | 0.501  |

Table 13 | Higher ( $\uparrow$ ) is better. Spearman's  $\rho$  performance of models with and without fine-tuning (FT) on NAS. We test 1024 architectures for search space.

# **B.** Additional Experiments

### **B.1.** Limited Information Scenario

As mentioned in Section 4, despite the CodeNet dataset not displaying inputs to the code submissions, it is still possible to predict memory consumption via shared questions from both training and test time. We demonstrate this is also the case for APPS in Table 14, where omitting the problem statement (containing input information) does not significantly harm predictions (only a drop of  $0.08 \, \rho$ ) for code latency.

| RLM Input                | Spearman $\rho$ |
|--------------------------|-----------------|
| Problem + Code (Default) | 0.93            |
| Code Only                | 0.85            |

Table 14 | Higher ( $\uparrow$ ) is better. Spearman  $\rho$  for when the model is trained over problem and code (default setting), vs. observing the code submission only. We test 1024 programs per language.

### **B.2.** Ranking

Continuing from Figure 3, we also provide further evidence that the RLM is capable of selecting the lowest latency (i.e. fastest) code submissions for a given question on APPS. In many cases, top-1 identification can be impossible as there are numerous submissions with very similar or identical implementations. For example, one maximum-subarray question in APPS has 4 out of 20 submissions using exactly the same "Kadane's algorithm" (Bentley, 1984). Instead, we vary the top-x% in Figure 10, to show that the RLM can at least identify the top percentile of submissions in general.

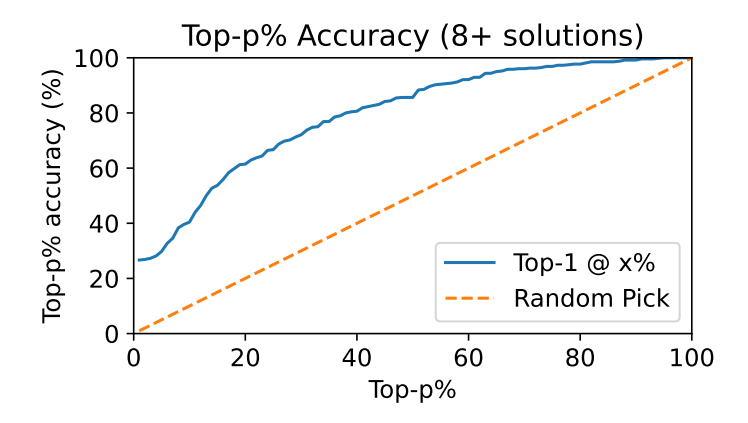


Figure 10 | Higher ( $\uparrow$ ) is better. Fraction of problems (with >8 solutions) where the model's predicted best solution lies within the true top-p% of solutions; dashed line shows the random pick baseline.

# C. Experimental Settings

We use the codebase from https://github.com/google-deepmind/regress-lm to train the RLM. We use the following default hyperparameters:

- Optimization and schedule. We use Adafactor. Pretraining uses a learning rate of  $1\times10^{-3}$ ; fine-tuning uses  $5\times10^{-5}$ . Gradients are clipped at a global norm of 2.0. The scheduler is a linear warmup for the first 10% of steps followed by cosine decay.
- **Decoder sizes:** We match the corresponding T5Gemma model where mentioned. Otherwise, we use two decoder layers, with hidden-sizes 2048 for both attention (with 8 heads) and feedforward.
- **Inference:** We take the median of 64 samples from the decoder for our pointwise estimate. The sample size can be increased to produce even more accurate pointwise predictions, but we found this default was sufficient.
- **Input length:** Our encoder uses a maximum of 2048 token lengths, and crops any tokenization sequences beyond this limit. Truncation only occurred for ONNX graphs from NAS data, but this does not significantly harm performance (as seen in Table 8) as cell structures repeat throughout the architecture.

# D. Data: Extended

# D.1. y-Value Distributions

In Figure 11, we plot the histogram of all y-values encountered in the datasets. This is to demonstrate the wildly different value ranges both across and within datasets, ranging from  $10^{-1}$  to  $10^{5}$  orders of magnitude. We emphasize that these ranges would make training using an MSE-based loss incredibly difficult, due to the sheer amount of variability of per-example loss magnitudes, and tedious normalizations to be performed per dataset.

This further highlights the necessity and benefit of using (1) cross-entropy as the loss for each example is well-behaved and (2) decoder head which does not require any *y*-normalizations.

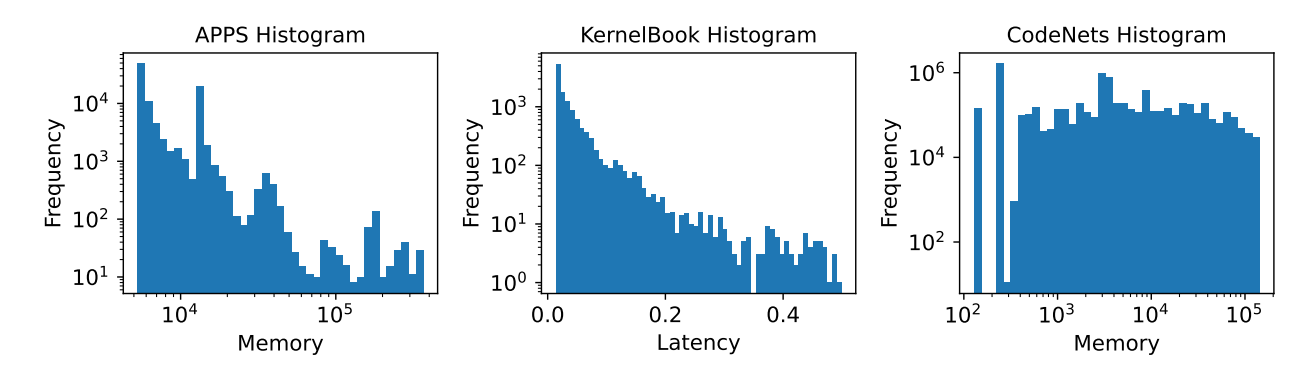


Figure 11 | Histogram of the target values for APPS, KernelBook and CodeNet

### D.2. Extra Leetcode Data for APPS

As a small aside, in APPS, we also appended additional 600 examples from EffiBench (Huang et al., 2025), another set of Leetcode problems and submissions. For each problem, generate\_test\_case() provides the inputs and expected output, and we measure the wall-clock time of repeatedly running the solution on these cases, averaging over many iterations and trials.

### D.3. Generating the SNAS Dataset

We construct the SNAS dataset by repeatedly sampling, briefly training, and recording lightweight CNN architectures on CIFAR-10 under a fixed-budget protocol:

- Sampling. For each example, we draw a macro configuration (e.g., stem width, stacks, cells per stack, width multiplier) and a micro cell DAG with operations from a small registry; residual connections may be enabled. The resulting network is serialized to a compact, reconstructable arch\_str.
- Training & evaluation. Each sampled network is trained for a small, fixed budget (steps or wall time) using SGD with momentum and a cosine learning-rate schedule under mixed precision (FP16/BF16). Augmentation and normalization follow standard CIFAR-10 practice and are executed on-GPU (8 Nvidia A6000 and 5 3090 GPUs). We report top-1 accuracy on a held-out evaluation subset of the test split.
- Logging. We stream one JSONL record per architecture with uid, val\_accuracy (primary label), params, train\_time\_sec, steps\_ran, precision, batch\_size, and arch\_str.

# D.4. Hardware Profiling

Below, we discuss specific details on how we collected y-values for varying code datasets.

### D.4.1. APPS

We use the following system configuration to profile problems from the APPS Hendrycks et al. (2021) dataset.

- **CPU:** AMD EPYC 7702 ("Rome"), 1× socket, 64 cores / 128 threads (SMT enabled); boost enabled; frequency range ~1.50–2.18 GHz.
- **Topology & Caches:** L1d: 2 MiB total (64 instances); L1i: 2 MiB total (64 instances); L2: 32 MiB total (64 instances); L3: 256 MiB total (16 slices).
- NUMA: Single node (node0 CPUs 0-127).
- Memory: 503 GiB RAM (no swap configured).
- OS/Kernel: Ubuntu 22.04, Linux 6.8.0-45-generic (x86\_64).

We profile Python solutions from the APPS train split with a small wrapper and consistent run protocol; the primary metric is dyn peak alloc bytes.

- For each problem, load solutions. json and input output. json.
- Execution modes. If fn\_name exists, run in *callable* mode by passing JSON args; otherwise run as *stdin* program. Each run executes in a fresh Python process with -I -S -B.
- Wrapper basics. Pre-import common stdlib modules, raise recursion limit, keep site-packages importable under -I/-S, set PYTHONHASHSEED=0. Outputs are discarded during timing.
- Warmup & repeats. Per (solution, input): discard warmup runs (default 3), then measure repeats (default 11). Per-run timeout: 10s.
- Timing. Wall time: perf\_counter\_ns. CPU time (POSIX): RUSAGE\_CHILDREN deltas.
- Dynamic memory (primary). Via tracemalloc, one untimed instrumented run per solution collects dyn\_peak\_alloc\_bytes, dyn\_alloc\_bytes\_pos, and dyn\_alloc\_count\_pos (attributed to the user file). One ru\_maxrss collects dyn\_rss\_peak\_bytes. Lightweight trace/profile counters (line events, call count, max depth) are also recorded.
- **Output.** We write one CSV row per (solution,input set) with summary stats (min/median/mean/p90/max/stddev/variance) for wall and CPU time, run counts, Python version, host, UTC timestamp, and the dynamic metrics above.

We report dyn\_peak\_alloc\_bytes (from tracemalloc) as our primary memory metric because it isolates Python-heap usage; peak RSS (dyn\_peak\_alloc\_bytes) is provided as a secondary, noisier indicator capturing native allocations (e.g., NumPy) and allocator effects. This emphasizes Python-level memory complexity while still flagging cases dominated by non-Python memory. Our target for the RLM is dyn\_peak\_alloc\_bytes.

### D.4.2. KernelBook

We use the following system configuration for KernelBook Paliskara & Saroufim (2025) A6000 profiling.

• **CPU:** Intel Xeon Gold 6448Y, 2× sockets, 64 cores / 64 threads (SMT disabled); boost enabled; frequency range ~0.80–2.10 GHz.

- **Topology & Caches:** L1d: 3 MiB total (64 instances); L1i: 2 MiB total (64 instances); L2: 128 MiB total (64 instances); L3: 120 MiB total.
- NUMA: Two nodes (node0 CPUs 0-31; node1 CPUs 32-63).
- Memory: 1008 GiB RAM; 4 GiB swap.
- **GPU/Driver:** 1× NVIDIA RTX A6000 (48 GiB), driver 530.30.02; CUDA 12.1.

We profile each Triton kernel from KernelBook on a single NVIDIA A6000. After a short JIT warmup, we time an adaptive loop seeded at 20 iterations and extended to a  $\geq 1$  s window; this window is repeated for 5 trials. We report median latency (ms) and also record the across-trial standard deviation.

For inputs, we use the dataset-provided constructors and activations, automatically trying a small set of argument orderings (parameters first, activations first, and interleavings) and using the first that passes shape checks. Per kernel, we write [index, sha, latency\_ms, stddev\_ms] to CSV and continue past failures (e.g., OOM or shape mismatch) without aborting the run.

# D.5. Triton Code Sample (KernelBook)

### Triton Kernel Example #4949; Latency (0.0152 ms) 1 import torch 2 import triton 3 import triton.language as tl 4 from torch.\_inductor.runtime.triton\_heuristics import grid 5 from torch.\_C import \_cuda\_getCurrentRawStream as get\_raw\_stream from torch.\_inductor.runtime import triton\_helpers 7 from torch import nn 8 assert\_size\_stride = torch.\_C.\_dynamo.guards.assert\_size\_stride empty\_strided\_cuda = torch.\_C.\_dynamo.guards.\_empty\_strided\_cuda 12 Otriton.jit 13 def triton\_per\_fused\_add\_div\_mul\_rsub\_sum\_0(in\_out\_ptr0, in\_ptr0, in\_ptr1, 14 xnumel, rnumel): XBLOCK: tl.constexpr = 1 RBLOCK: tl.constexpr = 256 xoffset = tl.program\_id(0) \* XBLOCK tl.full([1], xoffset, tl.int32) 18 19 tl.full([RBLOCK], True, tl.int1) rindex = tl.arange(0, RBLOCK)[:] tl.full([RBLOCK], True, tl.int1) 21 r0 = rindextmp0 = tl.load(in\_ptr0 + r0, None) tmp1 = tl.load(in\_ptr1 + r0, None) 24 tmp2 = tmp0 \* tmp1tmp3 = tl.broadcast\_to(tmp2, [RBLOCK]) 26 tmp5 = triton\_helpers.promote\_to\_tensor(t1.sum(tmp3, 0)) 27 tmp6 = tl.broadcast\_to(tmp0, [RBLOCK]) 28 29 tmp8 = triton\_helpers.promote\_to\_tensor(tl.sum(tmp6, 0)) 30 tmp9 = tl.broadcast\_to(tmp1, [RBLOCK]) tmp11 = triton\_helpers.promote\_to\_tensor(tl.sum(tmp9, 0)) tmp12 = 2.0tmp13 = tmp5 \* tmp12tmp14 = 1.034 tmp15 = tmp13 + tmp1436 tmp16 = tmp8 + tmp11tmp17 = tmp16 + tmp14tmp18 = tmp15 / tmp1738 tmp19 = tmp14 - tmp1839 40 tl.debug\_barrier() 41 tl.store(in\_out\_ptr0 + tl.full([1], 0, tl.int32), tmp19, None) 42 43 def call(args): arg0\_1, arg1\_1 = args 45 46 args.clear() assert\_size\_stride(arg0\_1, (4, 4, 4, 4), (64, 16, 4, 1)) assert\_size\_stride(arg1\_1, (4, 4, 4, 4), (64, 16, 4, 1)) 47 48 49 with torch.cuda.\_DeviceGuard(0): torch.cuda.set\_device(0) buf0 = empty\_strided\_cuda((), (), torch.float32) buf3 = buf0del buf0 get\_raw\_stream(0) triton\_per\_fused\_add\_div\_mul\_rsub\_sum\_0[grid(1)](buf3, arg0\_1, arg1\_1, 1, 256, num\_warps=2, num\_stages=1) 56 57 del arg0\_1 del arg1\_1 58 59 return buf3,

# Triton Kernel Example #4949; Latency (0.0152 ms) 1 lass DiceLossNew(nn.Module): 2 def \_\_init\_\_(self, weight=None, size\_average=True): 4 super(DiceLossNew, self).\_\_init\_\_() 5 def forward(self, input\_0, input\_1): 7 arg0\_1 = input\_0 8 arg1\_1 = input\_1 9 output = call([arg0\_1, arg1\_1]) 10 return output[0]

### D.6. ONNX Graph Code Sample

```
ONNX Graph (SNAS Architecture #10. Accuracy: 60.93%)
\leftrightarrow features.0.bn.weight[FLOAT, 16] %features.0.bn.bias[FLOAT, 16] %features.0.bn.\leftrightarrow

→ running_mean[FLOAT, 16]  %features.0.bn.running_var[FLOAT, 16]  %features.1.ops.1.⇔

                 → weight[FLOAT, 6x1x7x7] %features.1.ops.1.op.2.weight[FLOAT, 6x6x1x1] %features.1.ops.1. ↔ op.3.weight[FLOAT, 6] %features.1.ops.1.op.3.bias[FLOAT, 6] %features.1.ops.1.op.3... ↔ running_mean[FLOAT, 6] %features.1.ops.1.op.3.running_var[FLOAT, 6] %features.1.ops.1... ↔

    ∴ conv.weight[FLOAT, 6x6x1x1]    %features.1.ops.2.bn.weight[FLOAT, 6]    %features.1.ops.2.bn

                  → .bias[FLOĀT, 6] %features.1.ops.2.bn.running_mean[FLOĀT, 6] %features.1.ops.2.bn.←

→ running_var[FLOAT, 6] % features.1.ops.3.conv.conv.weight[FLOAT, 6x6x3x3] % features.1.

                → running_var[FLOAT, o] %reatures.1.ops.3.conv.weight[FLOAT, 6x6x3x3] %teatures.1. ↔ ops.3.conv.bn.weight[FLOAT, 6] %features.1.ops. ↔ .3.conv.bn.running_mean[FLOAT, 6] %features.1.ops.3.conv.bn.running_var[FLOAT, 6] % ← features.1.ops.4.op.1.weight[FLOAT, 5x1x3x3] %features.1.ops.4.op.2.weight[FLOAT, 5x5x1x ← 1] %features.1.ops.4.op.3.weight[FLOAT, 5] %features.1.ops.4.op.3.bias[FLOAT, 5] % ← features.1.ops.4.op.3.running_mean[FLOAT, 5] %features.1.ops.4.op.3.running_var[FLOAT, 5 ← 1x1x2x2] %feature
                                   %features.1.ops.4.op.5.weight[FLOAT, 5x1x3x3]
\%/features/features.8/ops.1/act/Relu\_output\_0 = \frac{Relu}{\%}/features/features.8/ops.1/op/Max \leftrightarrow \frac{Relu}{\%}/features/features/features/features/features/features/features/features/features/features/features/features/features/features/features/features/features/features/features/features/features/features/features/features/features/features/features/features/features/features/features/features/features/features/features/features/features/features/features/features/features/features/features/features/features/features/features/features/features/features/features/features/features/features/features/features/features/features/features/features/features/features/features/features/features/features/features/features/features/features/features/features/features/features/features/features/features/features/features/features/features/features/features/features/features/features/features/features/features/features/features/features/features/features/features/features/features/features/features/features/features/features/features/features/features/features/features/features/features/features/features/features/features/features/features/features/features/features/features/features/features/features/features/features/features/features/features/features/features/features/features/features/features/features/features/features/features/features/features/features/features/features/features/features/features/features/features/features/features/features/features/features/features/features/features/features/features/features/features/fe
                  → Pool_output_0) %/features/features.8/ops.2/op/op.0/Relu_output_0 = Relu(%/features/

    features.8/ops.1/act/Relu_output_0) %/features/features.8/ops.2/op/op.1/Conv_output_0 = 
    Conv[dilations = [1, 1], group = 32, kernel_shape = [3, 3], pads = [1, 1, 1, 1], strides ←
    Conv[dilations = [1, 1], group = 32, kernel_shape = [3, 3], pads = [1, 1, 1, 1], strides ←
    Conv[dilations = [1, 1], group = 32, kernel_shape = [3, 3], pads = [1, 1, 1, 1], strides ←
    Conv[dilations = [1, 1], group = 32, kernel_shape = [3, 3], pads = [1, 1, 1, 1], strides ←
    Conv[dilations = [1, 1], group = 32, kernel_shape = [3, 3], pads = [1, 1, 1, 1], strides ←
    Conv[dilations = [1, 1], group = 32, kernel_shape = [3, 3], pads = [1, 1, 1, 1], strides ←
    Conv[dilations = [1, 1], group = 32, kernel_shape = [3, 3], pads = [1, 1, 1, 1], strides ←
    Conv[dilations = [1, 1], group = 32, kernel_shape = [3, 3], pads = [1, 1, 1, 1], strides ←
    Conv[dilations = [1, 1], group = 32, kernel_shape = [3, 3], pads = [1, 1, 1, 1], strides ←
    Conv[dilations = [1, 1], group 

→ group = 1, kernel_shape = [1, 1], pads = [0, 0, 0, 0], strides = [1, 1]] (%/features/←)
                   \rightarrow \texttt{features.8/ops.2/op/op.1/Conv\_output\_0}, \ \texttt{\%features.8.ops.2.op.2.weight)} \ \ \texttt{\%/features/} \\ \leftarrow \\ \texttt{1.2.0} 
                  → features.8/ops.2/op/op.3/BatchNormalization_output_0 = BatchNormalization[epsilon = 9.999↔

→ 99974737875e-06, momentum = 0.899999976158142] (%/features/features.8/ops.2/op/op.2/↔)

                  = {\tt Relu(\%/features/features.8/ops.2/op/op.3/BatchNormalization\_output\_0)} \quad \% {\tt features.8/} \leftarrow {\tt res.2.6} \\
                   \hookrightarrow ops.2/op/op.5/Conv_output_0 = Conv[dilations = [1, 1], group = 32, kernel_shape = [3, 3], \leftrightarrow

→ pads = [1, 1, 1, 1], strides = [1, 1]](%/features/features.8/ops.2/op/op.4/Relu_output_0↔)

                            , \% features.8.ops.2.op.5.weight) \%/features/features.8/ops.2/op/op.6/Conv_output_0 = \leftrightarrow

    → ) %/features/features.8/ops.2/op/op.7/BatchNormalization_output_0 = BatchNormalization[

                  → epsilon = 9.99999974737875e-06, momentum = 0.899999976158142] (%/features/features.8/ops.2↔
                  \hookrightarrow /op/op.6/Conv_output_0, %features.8.ops.2.op.7.weight, %features.8.ops.2.op.7.bias, %\hookleftarrow
                   \leftarrow \texttt{features.8.ops.2.op.7.running\_mean}, \\ \text{ $\%$ features.8.ops.2.op.7.running\_var) } \\ \text{ $\%$ features.} 
                   \hspace{2cm} \hookrightarrow \hspace{2cm} \texttt{Concat\_output\_0}, \hspace{2cm} \texttt{\%} features.8.input\_proj.3.conv.weight) \hspace{2cm} \texttt{\%} / features/features.8 / input\_proj. \\ \leftarrow \hspace{2cm} \texttt{Concat\_output\_0}, \hspace{2cm} \texttt{\%} features.8 / input\_proj. \\ \leftarrow \hspace{2cm} \texttt{Concat\_output\_0}, \hspace{2cm} \texttt{\%} features.8 / input\_proj. \\ \leftarrow \hspace{2cm} \texttt{Concat\_output\_0}, \hspace{2cm} \texttt{\%} features.8 / input\_proj. \\ \leftarrow \hspace{2cm} \texttt{Concat\_output\_0}, \hspace{2cm} \texttt{\%} features.8 / input\_proj. \\ \leftarrow \hspace{2cm} \texttt{Concat\_output\_0}, \hspace{2cm} \texttt{\%} features.8 / input\_proj. \\ \leftarrow \hspace{2cm} \texttt{Concat\_output\_0}, \hspace{2cm} \texttt{\%} features.8 / input\_proj. \\ \leftarrow \hspace{2cm} \texttt{Concat\_output\_0}, \hspace{2cm} \texttt{Conc

    → 3/bn/BatchNormalization_output_0 = BatchNormalization[epsilon = 9.99999974737875e-06, 

                   \hookrightarrow \texttt{features.8.input\_proj.3.bn.weight}, \ \ \text{\%} \texttt{features.8.input\_proj.3.bn.bias}, \ \ \text{\%} \texttt{features.8.} \leftarrow \\
                  → features.8/ops.3/op/AveragePool_output_0 = AveragePool[ceil_mode = 0, count_include_pad = → 0, kernel_shape = [3, 3], pads = [1, 1, 1, 1], strides = [1, 1]](%/features/features.8/↔ → input_proj.3/bn/BatchNormalization_output_0) %/features/features.8/ops.3/act/↔
                   → Relu_output_0 = Relu(%/features/features.8/ops.3/op/AveragePool_output_0)
%/features/features.8/Add_output_0 = Add(%/features/features.8/ops.2/op/op.7/↔

→ BatchNormalization_output_0, %/features/features.8/ops.3/act/Relu_output_0)
```

# ONNX Graph (SNAS Architecture #10. Accuracy: 60.93%)

```
%/features/features.8/ops.4/op/AveragePool_output_0 = AveragePool[ceil_mode = 0, \( \to \) \( \to \) count_include_pad = 0, kernel_shape = [3, 3], pads = [1, 1, 1, 1], strides = [1, 1]](%/\( \to \) features/features.8/Add_output_0) %/features/features.8/ops.4/act/Relu_output_0 = Relu(%\( \to \) \( \to \) features/features.8/ops.4/op/AveragePool_output_0) %/features/features.8/Concat_output_\( \to \) \( \to \) 0 = Concat[axis = 1](%/features/features.8/ops.3/act/Relu_output_0, %/features/features.8\( \to \) \( \to \) ops.4/act/Relu_output_0) %/GlobalAveragePool_output_0 = GlobalAveragePool(%/features/\( \to \) \( \to \) features.8/Concat_output_0) %/Flatten_output_0 = Flatten[axis = 1](%/\( \to \) \( \to \) GlobalAveragePool_output_0) %logits = Gemm[alpha = 1, beta = 1, transB = 1](%/\( \to \) \( \to \) Flatten_output_0, %classifier.weight, %classifier.bias) return %logits}
```

# D.7. Example Code Submissions

# Problem (Maximum Subarray Sum with One Deletion)

Given an integer array arr, return the maximum sum of a non-empty subarray after optionally deleting at most one element from that subarray (the result must still be non-empty).

# Memory-efficient (O(1) extra space) from typing import List class Solution: def maximumSum(self, arr: List[int]) -> # keep: best sum with no deletion # drop: best sum with one deletion keep = arr[0] drop = float('-inf') ans = arr[0]for x in arr[1:]: # delete current x OR already deleted drop = max(drop + x, keep)# Kadane keep = max(keep + x, x)ans = $\max$ (ans, keep, drop) return ans

```
Less memory-efficient
from typing import List
class Solution:
  def maximumSum(self, arr: List[int]) ->
    # extra memory overhead
    max_res = [0] * len(arr)
    max_start = [0] * len(arr)
    max_{end} = [0] * len(arr)
    for i. n in enumerate(arr):
      \max_{i} = n \text{ if } i == 0 \text{ else } \max(n, i)
     max_end[i-1] + n)
    # debug overhead
    print(max_end)
    # materialize reverse pass array
    for i, n in list(enumerate(arr))[::-1]:
      max_start[i] = n if i == len(arr) -
    1 else max(n, max_start[i+1] + n)
    # debug overhead
    print(max_start)
    for i, n in enumerate(arr):
     left = n if i == 0 else max_end[i
    -17
     right = n if i == len(arr) - 1 else
    max_start[i+1]
     max_res[i] = max(left, right, left +
     right)
    # debug overhead
    print(max_res)
    return max(max_res)
```

Figure 12 | LeetCode "Maximum Subarray Sum with One Deletion". (Left): one-pass DP that keeps only two running states (keep, drop)—O(1) extra space and O(n) time. (Right): builds three length-n arrays (max\_end, max\_start, max\_res)—O(n) extra space and O(n) time. Ground truth memory: O(1) version 5608 bytes; less memory-efficient version 7136 bytes. RLM predictions: 5549 and 6228 bytes, respectively. The gap comes from (i) storing three auxiliary arrays of size n, (ii) materializing list(enumerate(arr)) for the reverse pass, and (iii) debug print(...) calls that create large temporary strings when printing full arrays.

# Problem (Maximum Sum Circular Subarray)

Given an integer array A that represents a circular array, return the maximum possible sum of a non-empty subarray of the circular array. Wrap-around is allowed, but each element of the fixed buffer A may be used at most once in the subarray.

### Memory-efficient (O(1) extra space)

```
from typing import List
class Solution:
  def maxSubarraySumCircular(self, A: List
    [int]) -> int:
    # scalar accumulators O(1) space
   maxsum = minsum = A[0]
    # rolling state; no array alloc
    curmax = curmin = total = 0
   for num in A:
      # Kadane step for max
      curmax = max(num, curmax + num)
      maxsum = max(maxsum, curmax)
      # Min-Kadane
      curmin = min(num, curmin + num)
      minsum = min(minsum, curmin)
      # single pass accumulation
     total += num
    # computed from scalars; (O(1))
    return max(maxsum, total - minsum) if
    maxsum > 0 else maxsum
```

# Less memory-efficient (O(n) extra space)

```
from typing import List
class Solution:
  def maxSubarraySumCircular(self, A: List
    [int]) -> int:
    def maxSubarray(A: List[int]) -> int:
      # length-n DP array (O(n))
      dp = [0] * len(A)
      dp[0] = A[0]
      for i in range(1, len(A)):
        dp[i] = max(A[i], dp[i - 1] + A[i])
      # entire DP history to take max
      return max(dp)
    temp = maxSubarray(A)
   res = float('-inf')
    # allocates rightMax (length-n)
   rightMax = [max(A[0], 0)] + [0] * (len
    (A) - 1)
    currMax = max(A[0], 0)
    \# prefix-tracking with rightWin
   rightWin = [A[0]] + [0] * (len(A) - 1)
    for idx. x in enumerate(A[1:]):
     currMax
                    = max(x + rightWin[idx
    ], currMax)
      rightMax[idx+1] = currMax
      rightWin[idx+1] = x + rightWin[idx]
    # extra full pass
    A.reverse()
    # suffix-sum with leftWin
   leftWin = [A[0]] + [0] * (len(A) - 1)
    for idx, x in enumerate(A[1:]):
      leftWin[idx + 1] = x + leftWin[idx]
      currMax = rightMax[len(A) - idx - 2]
      res = max(res, currMax + leftWin[idx
    ])
    return max(res, temp)
```

Figure 13 | Side-by-side solutions for the circular maximum subarray problem. Both run in *O*(*n*) time. (**Left**) (**O**(1) space) tracks only scalar accumulators (Kadane for max and min + total), which avoids auxiliary arrays. (**Right**) (**O**(n) space) allocates several length-*n* arrays (dp, rightMax, rightWin, leftWin) and also reverses A in place, increasing memory usage. RLM memory footprint estimated: **5634** (left, more memory-efficient) vs. **6430** (right, less memory-efficient). (Ground truth: **5508** and **6528**, respectively.)

# Problem (Array of Doubled Pairs)

Given an integer array A of even length, return True iff it is possible to reorder it so that  $A[2i+1] = 2 \cdot A[2i]$  for every  $0 \le i < |A|/2$ .

**Constraints:**  $0 \le |A| \le 3 \times 10^4$ , |A| is even,  $-10^5 \le A[i] \le 10^5$ .

# More memory-efficient from typing import List class Solution: def canReorderDoubled(self, A: List[int]) -> bool # re-usable frequency map $D = \{\}$ for x in A: D[x] = D.get(x, 0) + 1# sort keys once D = dict([kv for kv in sorted(list(D. items()), key= lambda x: x[0])]) # in-place pairs by # updating counts for x in D: while D[x] > 0: D[x] = 1**if** x <= 0: $pair_x = x / 2$ else: $pair_x = x * 2$ if D.get(pair\_x, 0) > 0: D[pair\_x] -= 1 else: return False return True

```
Less memory-efficient
from typing import List
from collections import Counter
class Solution:
 def canReorderDoubled(self, A: List[int])
     -> bool:
    # initialize three lists (O(n))
   negs = [a for a in A if a < 0]
   pos = [a for a in A if a > 0]
    zero = [a for a in A if a == 0]
    if any(map(lambda x: len(x) % 2 != 0, [
    negs, pos, zero])):
     return False
    if not self.is_valid(negs, True) or
    not self.is_valid(pos, False):
      return False
   return True
  def is_valid(self, A, neg=False):
   # sorted copy per bucket
    A = sorted(A)
    if neg:
      # list reverse duplicated
      A = A[::-1]
    # extra Counter (hash map)
    c = Counter(A)
    for a in A:
      if c[a] == 0:
        continue
      target = a * 2
      if c[target] == 0:
        return False
      c[a] -= 1
      c[target] -= 1
    return True
```

Figure 14 | Side-by-side solutions to the problem. (Left) builds a single frequency map and reuses it while pairing, avoiding three full partitions (negs/pos/zero), extra sorted copies, and multiple Counter objects. RLM estimated memory footprint was 6518. (Right) materializes three lists, sorts (and reverses) sublists, and constructs Counters inside validation passes, increasing allocations and peak live objects. RLM estimated memory footprint: 10197. (Ground truth: 6178 and 10588, respectively.)